IEEE Instrumentation and Measurement
Technology Conference
Budapest, Hungary, May 21-23, 2001

A Gain-Scheduling PID-like Controller for Peltier-Based Thermal Hysteresis Characterization Platform

A.M.N. Lima[1], G.S. Deep[1], L.A.L. de Almeida[1,2], H. Neff[1] and M. Fontana[1]
[1]Departamento de Engenharia Elétrica - Universidade Federal da Paraíba - Campus II,
Caixa Postal 10.004 - CEP 58109-970 - Campina Grande - PB - Brazil
e-mail: {amnlima,deep,helmut,marcio}@dee.ufpb.br
[2]Departamento de Engenharia Elétrica - Universidade Federal da Bahia
R. Aristides Novis, 2 - Federação - CEP 40210-630 - Salvador - BA - Brazil
e-mail: lalberto@ufba.br

Abstract *– A linearized dynamic model for thermoeletric modules has been proposed and validated using experimental data. Employing this model, a digital temperature controller for sinusoidal thermal cycling of a vanadium-dioxide microbolometer has been designed. The controller permits the rate of change of temperature varying over a wide range with a tolerance of 0.01C.*

Keywords *– Thermoelectricity, Temperature control, Bolometers, Vanadium compounds, Thermal hysteresis*

I. INTRODUCTION

Thin film of vanadium dioxide (VO_2) exhibits large variation of its electrical resistance with temperature. This makes the material an ideal candidate towards the design of sensitive, uncooled microbolometric radiation detectors [1], [2]. Thermodynamical characterization of VO_2 thin films demands a precise and flexible temperature control. The reason for requirement relies on strong temperature-history dependent of the thermal features of these devices. Different hysteresis loops are produced by cycling the sample following different thermal paths. Thus, undesirable small temperature oscillations, caused by the temperature controller, can corrupt the VO_2 characteristics. The self-organization of the film's microcrystals, at very low-rate cycling, can drive the sensor behaviour into anomalous (Fig. 1a) or chaotic regimes [3]. This anomalous behavior occurs under special conditions, and the experiment would require human observation and intervention during its realization in order to analyze and identify the trigger conditions for chaos. Thus, the controller should provide repeatable long term temperature cycling to force the device to visit major and minor hysteresis loops [4] (Fig. 1b), while maintaining small closed-loop temperature oscilations.

For the case of VO_2 characterization, the closed-loop oscilations should be maintained within less than $\pm 0.05°C$ in the temperature range of $+20°C$ to $+80°C$, for arbitrary reference temperature excitation. To achieve a proper controller design meeting these requirements, it is necessary to use a thermoelectric cooler/heater.

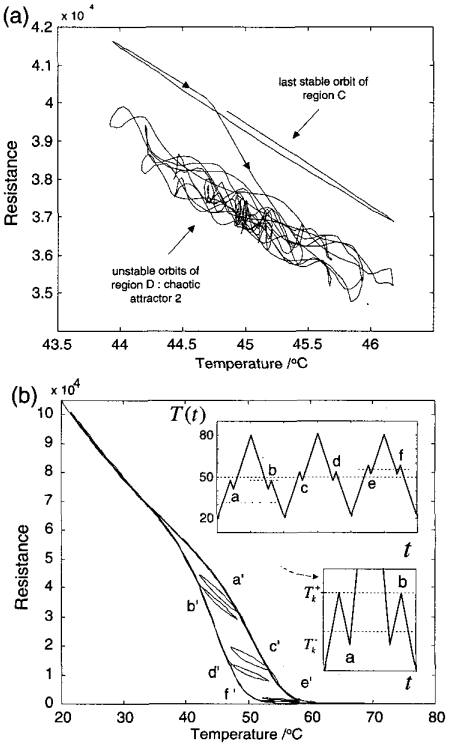

Fig. 1. The typical $R \times T$ characteristics of the VO_2 thin film.

The design of temperature controllers based on thermoeletric modules was investigated in [5], [6]. In [5] the temperature control problem has been addressed using digital controllers but no indication about the capability of tracking time-varying reference temperature were provided. In [6] a temperature controller with disturbance-rejection properties, based on a linear model for the thermoelectric module, including the heat sink, has been employed. The analysis of the experimental results presented in [6] revealed that the achieved closed-loop temper-

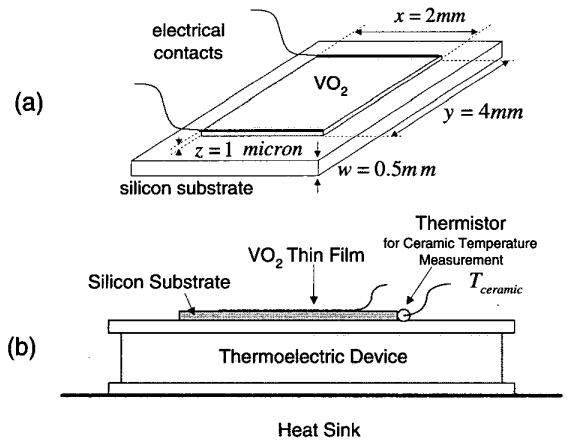

Fig. 2. (a) The sensor physical dimensions. (b) the film fixed on the Peltier module. (c) the thermal chamber: VO_2 film and Peltier module.

ature oscillations lies around $\pm 0.1°C$ which does not meet the requirements of our experiment.

In this paper we propose a continuous-time linearized model for the thermoelectric module, including the heat sink and the thermal load. The design of the PID-like controller is based on this linearized model and we also propose a gain-schedule technique for the controller, based on the gain of the linearized model. To implement the this structure, a microcomputer-based VO_2 thin film sensor characterization platform with IEEE-488 interface employing laboratory equipment was used.

II. THE THERMAL CHAMBER

The VO_2 thin film sample used in our experiments has thickness of 1000Å that were sputtered onto a 100 oriented semi-insulating Si-substrate as shown in Fig. 2a. The sample has been mounted onto a thermoelectric module, inside an isolated thermal chamber (Fig. 3). Film temperature was measured using a very small thermistor (Fig. 2b). A digital controller (Fig. 4), implemented in an IEEE-488 environment (Fig. 5) was built to establish a high precision ramping of the temperature with the rate varying within the range $10°C$/min to $0.01°C$/min for arbitrary reference temperature ($+20°C$ to $+80°C$). A voltage-to-current converter is employed to provide the thermoeletric module excitation.

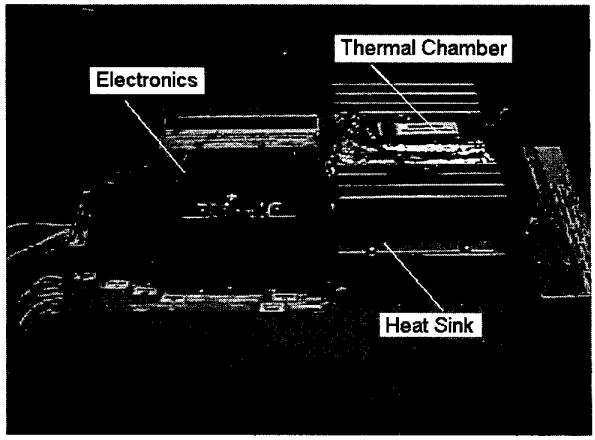

Fig. 3. Experimental prototype

To properly design a PID-like controller, it is often necessary to have a model for the plant under control. The thermal chamber can be considered to be constituted of three dynamic subsystems (Fig. 4). These dynamic systems comprise the complete thermal chamber model, as described in the following:

Module 1 The transfer function $H_{VO_2}(s)$ represents the dynamical behaviour of the VO_2 silicon substrate (Fig. 2a and 2b). It can be interpreted in terms of the effect on the film resistance as a result of a change in the temperature of the cold side T_c. This transfer function is assumed to be of first order and given by

$$H_{VO_2}(s) = (1/C_{sub}) \frac{1}{s + G_{sub}/C_{sub}}$$

where C_{sub} and G_{sub} are the thermal capacity and the heat transfer coefficient between substrate and cold side of the thermoelectric module, respectively;

Module 2 The transfer function $H_M(s)$ represents the dynamical behaviour of the thermistor. It can be interpreted in terms of the effect in the thermistor resistance as a result of changes in the temperature of the cold side T_c. This transfer function is assumed to be of first order and given by

$$H_M(s) = (1/C_t) \frac{1}{s + G_t/C_t}$$

where C_t and G_t are the thermal capacity and the thermal conductance of the thermistor, respectively;

Module 3 The combined thermoelectric and heat sink model $H_{TE}(s)$ is grouped with the thermistor model $H_M(s)$ to form the plant under control $H_{TE}(s)H_M(s)$. It is desired that the measured temperature $T_M(t)$ (Fig. 4) be the same as the film temperature $T_{VO_2}(t)$. Then, the time constant $\tau_{sub} = G_{sub}/C_{sub}$ of $H_{VO_2}(s)$ should be approximately the same as the time constant $\tau_t = G_t/C_t$ of $H_M(s)$ to avoid distortions of the hysteresis curve;

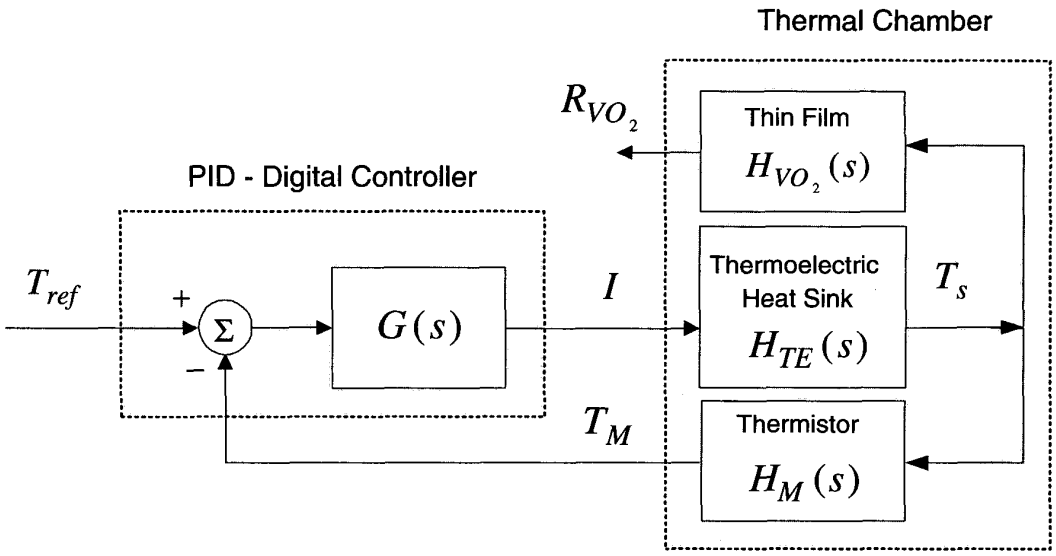

Fig. 4. Block diagram of the control system.

III. THE MODEL FOR THE THERMOELECTRIC MODULE AND HEAT-SINK

A thermoelectric or Peltier module is a semiconductor-based electronic component that functions as a small heat pump. By applying a direct current to the thermoelectric module, heat will be moved through the module from one side to the other. One module face, therefore, will be cooled while the opposite face simultaneously is heated. A change in the polarity of the current through the module will cause heat to be moved in the opposite direction.

There are a number of parameters associated with thermoelectric modules that normally would have to be considered in a mathematical model. To develop such a simplified model, we use an electrical equivalent model of the thermoelectric module .

To describe the physical system depicted in Fig. 2c and Fig. 6a we propose the electrical model shown in Fig. 6b. In this model, heat flow is represented by current flow, temperature difference by voltage, thermal conductance by electrical conductance and thermal capacity by electrical capacity. These parameters are defined as: G_s, G_h, G_m and G_c are respectively the thermal conductance $(W/^\circ K)$ of the heat sink to the surroundings, of the thermoelectric module hot side interface to the heat sink, of the thermoelectric module inner layer and of the thermoelectric module cold side interface to the thermal insulator; C_s the thermal capacity $(J/^\circ K)$ of the heat sink, C_h and C_c are respectively the thermal capacity the hot and cold sides; $P_h = \frac{I^2 R_m}{2} + \alpha T_h I$ is the heat power (W) at the hot side of the module, where α is the Seebeck coefficient $(V/^\circ K)$, I and R_m are the module electrical current (A) and ohmic module resistance (Ω) respectively, and T_h is the temperature of the hot side [7]; $P_c = \frac{I^2 R_m}{2} - \alpha T_c I$ is the heat power at the cold side and T_c is its temperature; T_a is the surrounding temperature.

Some considerations can be made to simplify the model described in Fig. 6b. The value of the heat sink capacity is considerably greater than the values of the heat capacity of the thermoelectric sides, $C_s >> C_h$ and $C_s >> C_c$. The thermal contact between the thermoelectric hot side and the heat sink is good enough to consider $G_h >> G_m$. The surrounding temperature T_a can be considered zero without loss of generality. With these considerations, the effect of the electrical heat P_R over the thermoelectric cold side temperature T_c can be approximated by the model described in Fig. 6c. A further consideration is that the time response of T_s resulted from an excitation P_R is much slower than the response time of T_c from an excitation P_c. In accordance with this, the effect of the heat flow at the thermoelectric cold side over its temperature T_c can be approximated by the model described in Fig. 6d. Using the latter model, we look for a transfer function to describe the the response of the cold side temperature T_c to an electrical input current I. Then, recalling that $P_c = \frac{I^2 R_m}{2} - \alpha T_c I$, we can realize a recurrent and nonlinear dependence on T_c.

To obtain a linear relation between T_c and I, additional considerations should be made. First, a small signal analysis turns to be more convenient to derive a transfer function. The thermoelectric operation is then restricted to a small region around $T_c = T_0$. A bias current I_0 is necessary to reach this tempera-

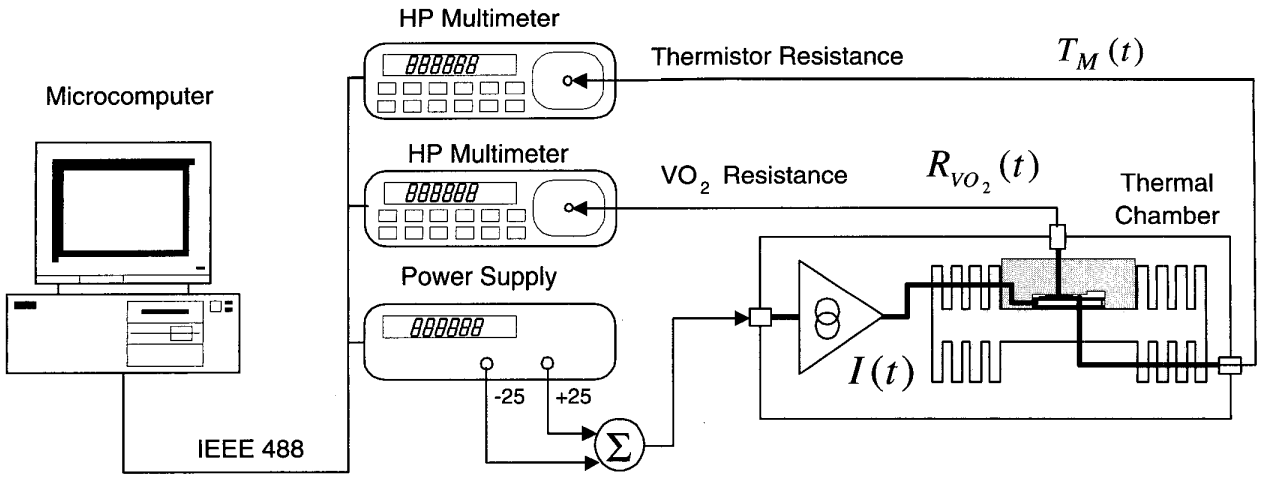

Fig. 5. Schematic of the VO_2 thermal characterization platform.

ture, and the current I can be represented as

$$I = I_0 + I_\delta$$

where I_δ is a current that represents the small signal excitation. At the operating point (I_0, T_0) we can define

$$\frac{\partial P_c}{\partial I_\delta} = R_m I_0 + R_m I_\delta - \alpha T_c \tag{1}$$

For small currents I_δ, we can consider $R_m I_\delta << (R_m I_0 - \alpha T_c)$ and (1) can be simplified to

$$\left.\frac{\partial P_c}{\partial I_\delta}\right|_{\substack{I=I_0 \\ T_c=T_0}} = R_m I_0 - \alpha T_0 \tag{2}$$

From (2) a linearized model with a dc gain that depends on the operating point (I_0, T_0), is obtained as the following transfer function

$$H_{TE}(s) = \frac{\Delta T_c(s)}{\Delta I(s)} = K_H \frac{(s+a)}{s^2 + sb + c} \tag{3}$$

where

$$K_H = \frac{1}{C_c}(R_m I_0 - \alpha T_0) \tag{4}$$

$$a = \frac{(G_m + G_s)}{C_s} \tag{5}$$

$$b = \frac{(C_c G_m + C_c G_s + G_c C_s + G_m C_s)}{C_c C_s} \tag{6}$$

$$c = \frac{G_m G_s + G_c G_m + G_c G_s}{C_c C_s} \tag{7}$$

The parameters of $H(s)$ obtained from experimental data are: $G_s = 0.83$, $G_m = 0.64$, $G_c = 0.05$, $C_s = 12$, $C_c = 0.5$, $\alpha = 0.05$ and $R_m = 1$. Thus, $H_{TE}(s)$ can be written using its numerical values as

$$K_H = 4I_0 - 0.1T_0, a = 0.12, b = 3, c = 0.1$$

IV. THE PID-LIKE CONTROLLER

Based on the linearized model derived in the previous section a PID-like controller can be designed to control the thermoelectric cooling/heating process. The transfer function of the PID-like controller is given by

$$G(s) = K_G \frac{s^2 + b_1 s + b_0}{s(s + a_1)} \tag{8}$$

The time constant of the thermistor τ_t can be neglected when compared with the equivalent time constant of $H_{TE}(s)$ and the closed-loop transfer function results

$$\frac{\Delta T_c(s)}{\Delta T_{ref}(s)} = \frac{G(s) H_{TE}(s)}{1 + G(s) H_{TE}(s)}$$

The calculations of K, b_1,b_0 and a_1 can be made using a pole-zero cancellation design methodology, for example. If pole-zero cancellation is employed $a_1 = a$, $b_1 = b$, $b_0 = c$ and consequently the closed-loop transfer function becomes

$$\frac{\Delta T_c(s)}{\Delta T_{ref}(s)} = \frac{K_G K_H}{s + K_G K_H}$$

In this case the closed-loop pole has been selected to be $-5b$ and thus

$$K_G = 5b / K_H$$

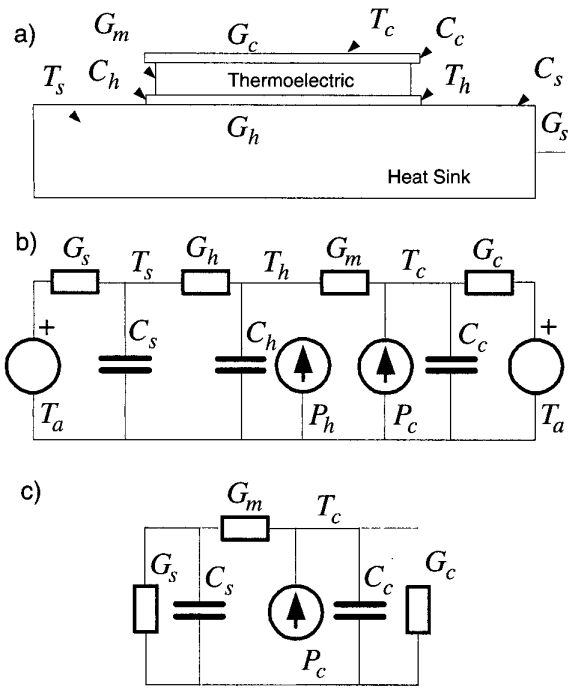

Fig. 6. Equivalent circuit representing the Peltier module and the heat-sink.

so that the pole placement does not change when K_H varies with the operating point. It is clear that the value of each calculated controller gain can vary with the operation point (I_0, T_0). This PID-like controller with gain scheduling has been implemented digitally on the IEEE-488 environment using standard laboratory equipments together with a microcomputer. The lowest sampling time achieved with this environment was about $0.3s$.

V. EXPERIMENTAL RESULTS

Thermoelectric module is limited in its maximum pumping capacity, which means that a certain model can theoretically reach a maximum temperature difference of ΔT between the two sides of the module. A standard single-stage thermoelectric cooling/heating module is capable of achieving a maximum no-load ΔT of approximately $70°C$. In our case, the maximum practical temperature difference obtained between the faces was $40°C$. This was due to the insufficient thermal isolation between the two sides as well the thermal loading. The thermoelectric module is mounted on a heat sink whose temperature fluctuates around $\pm 5°C$ relative to ambient temperature T_a. Considering $T_a = 30°C$, the temperature on the thermoelectric surface can vary from $-5°C$ to $+65°C$. This is unsuitable for a proper characterization of the device under test, which requires a temperature variation from $+20°C$ to $+80°C$. To raise the temperature beyond $+65°C$, additional heat can be produced by increasing the current I_0 and consequently the Joule heating $\frac{I^2 R_m}{2}$ term related to P_c. Even working beyond pumping capacity, the gain K_H is the same and the linear model (3) is still valid.

The linearized model of the thermoeletric model by suddenly changing the current $(0.1A)$ of the module and monitoring the temperature on the working side (see Fig. 7a). From this test we obtained the following values for the plant parameters: $K_H = 29.8$, $a = 0.12$, $b = 3$ and $c = 0.1$. The step response of the plant as per equation (3) agrees reasonably with the experimental curve.

In Fig. 7b is depicted the VO_2 film temperature with the use of the designed controller for a sinusoidal temperature reference. The initial overshoot (right inset of Fig. 7b) is due to a very large current step which takes the system to the nonlinear region. Accuracy of closed-loop control was determined to be $0.01°C$ (left inset of Fig. 7b) for rates varying from $10°C$/min to $0.01°C$/min .

VI. CONCLUSIONS

A linearized dynamic model of thermoeletric module around an operating has been experimentally determined. A feedback digital temperature controller based on this linearized model has been designed and implemented to be used as part of the characterization platform for VO_2 thin film micro-bolometer. A digital temperature controller for sinusoidal thermal cycling of this micro-bolometer, attached to the Peltier module, from $20°C$ to $80°C$ has been designed. The controller permits the rate of change of temperature varying over a wide range with a tolerance of 0.01C.

VII. ACKNOWLEDGMENTS

The authors thanks to CNPQ (Conselho Nacional de Desenvolvimento Científico e Tecnológico) and CAPES (Fundação Coordenação de Aperfeiçoamento de Pessoal de Nível Superior) for the award of research and study fellowship during the course of these investigations.

References

[1] V. Zerov, Y. Kulikov, V. Leonov, V. Malyarov, I. Khrebtov, and I. Shaganov, "Features of the operation of a bolometer based on a vanadium dioxide film in a temperature interval that includes a phase transition," *Journal of Optical Technology*, vol. 66, pp. 387–390, MAY 1999.

[2] C. Reintsema, E. Grossman, and J. Koch, "Improved VO_2 microbolometers for infrared imaging: operation on the semiconducting-metallic phase transition with negative electrothermal feedback," *SPIE Proceedings - Infrared Technology and Applications XXV*, vol. 3698, April 1999.

[3] L. de Almeida, G. Deep, A. Lima, and H. Neff, "Thermodynamics of thin VO_2 films within the hysteretic transition: Evidence for chaos near the percolation threshold," *Applied Physics Letter*, vol. 77, no. 26, pp. 4365–4367, 2000.

[4] L. de Almeida, G. Deep, A. Lima, H. Neff, and R. Freire, "A hysteresis model for vanadium oxide thermal radiation sensor," *Proceedings of the 17th IEEE Instrumentation and Measurement Technology Conference - IMTC*, May 2000.

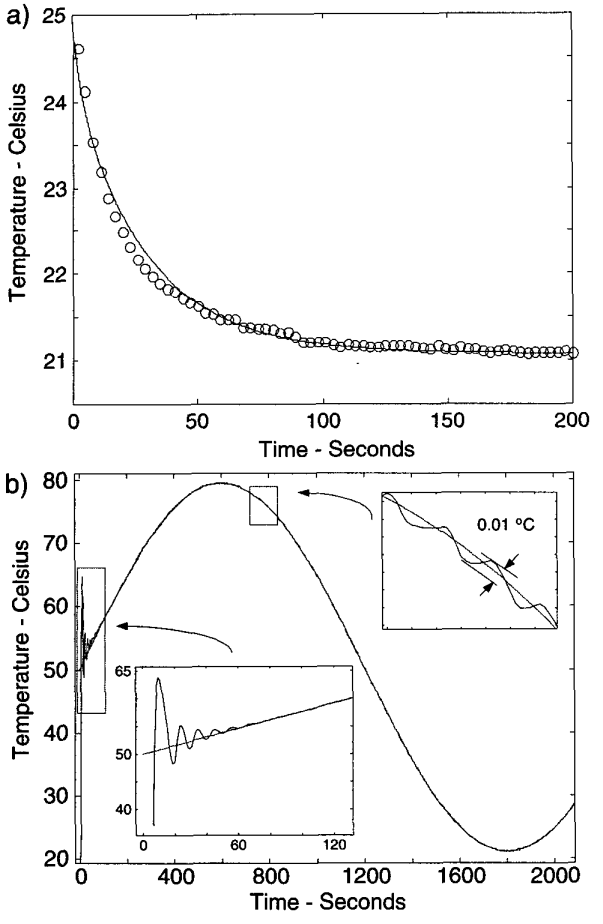

Fig. 7. a) Time response of the Peltier module for a current step of 0.1A. b) Closed-loop response for a sinusoidal temperature reference.

[5] P. Klinkhachorn, B. Huner, E. B. Overton, H. P. Dharmasena, and D. A. Gustowski, "A microprocessor-based piezoelectric quartz microbalance system for compound-specific detection," *IEEE Transactions on Instrumentation and Measurement*, vol. 39, pp. 264–268, February 1990.

[6] G. Festa and B. Neri, "Thermally regulated low-noise, wideband, I/V converter using peltier heat pumps," *IEEE Transactions on Instrumentation and Measurement*, vol. 43, pp. 900–905, December 1994.

[7] J. A. Chávez, J. A. Ortega, J. Salazar, A. Turó, and M. J. García, "Spice model of thermoelectric elements including thermal effects," *Proceedings of the 17th IEEE Instrumentation and Measurement Technology Conference - IMTC*, 2000.